

## Water Dynamics in Ionomer Membranes by Field-Cycling NMR Relaxometry

Jean-Christophe Perrin,<sup>\*,†</sup> Sandrine Lyonnard,<sup>†</sup> Armel Guillermo,<sup>†</sup> and Pierre Levitz<sup>‡</sup>*Structures et Propriétés d'Architectures Moléculaires, UMR 5819 (CEA-CNRS-UJF), DRFMC/SPRAM, CEA-Grenoble, 38054 Grenoble Cedex 9, France, and Laboratoire de Physique de la Matière Condensée, UMR 7643 du CNRS, Ecole Polytechnique, 91128 Palaiseau Cedex, France**Received: December 21, 2005; In Final Form: January 27, 2006*

The dynamic behavior of water within two types of ionomer membranes, Nafion and sulfonated polyimide, has been investigated by field-cycling nuclear magnetic relaxation. This technique, applied to materials prepared at different hydration levels, allows the proton motion on a time scale of microseconds to be probed. The NMR longitudinal relaxation rate  $R_1$  measured over three decades of Larmor angular frequencies  $\omega$  is particularly sensitive to the host–water interactions and thus well-suited to study fluid dynamics in restricted geometries. In the polyimide membranes, we have observed a strong dispersion of  $R_1(\omega)$  following closely a  $1/\sqrt{\omega}$  law in a low-frequency range (correlation times from 0.1 to 10  $\mu$ s). This is indicative of a strong interaction of water with “interfacial” hydrophilic groups of the polymeric matrix (wetting situation). Variations of the relaxation rates with water uptake reveal a two-step hydration process: solvation and formation of disconnected aqueous clusters near polar groups, followed by the formation of a continuous hydrogen bond network. On the contrary, in the Nafion we observed weak variations of  $R_1(\omega)$  at low frequencies. This is typical of a nonwetting behavior. At early hydration stages,  $R_1(\omega)$  evolves logarithmically, suggesting a confined bidimensional diffusion of protons in the microsecond time range. Such an evolution is lost at higher swelling where a plateau related to three-dimensional diffusion is observed.

## Introduction

Presently, ionomer membranes are extensively studied, notably for polymer electrolyte fuel cell (PEFC) applications. These membranes can be good ionic conductors when hydrated. The water management in a fuel cell during operation is one of the crucial problems to be solved; drying or flooding can arise from a noncontrolled competition between electro-osmosis and back diffusion of water molecules through the film. The necessity to operate the cell at a high water content when the membrane protonic conductivity is optimum and to do so at high temperatures possibly implies severe technological constraints (gas humidification, recycling of water produced at the cathode, hydration of the membranes when cycling the cell). The hydration state of the membranes is characterized by the number of water molecules per ionic group  $\lambda$ . A considerable effort has been made in the last years to understand the proton conduction processes as a function of  $\lambda$  and thus the water's role in enhancing conductivity, with the clear objective to improve the performance in view of further industrial applications.

Presently, the perfluorinated ionomer membranes stand as the best materials for PEFC applications; among them, the so-called Nafion is the most popular (Figure 1a). Its hydrophobic poly-(tetrafluoroethylene) backbone carries fluoroether side chains terminated by hydrophilic sulfonic acid groups. Although the Nafion exhibits remarkable performance and notably an unchallenged protonic conductivity under operating conditions in fuel cell power-supplied prototypes, it has numerous drawbacks (high

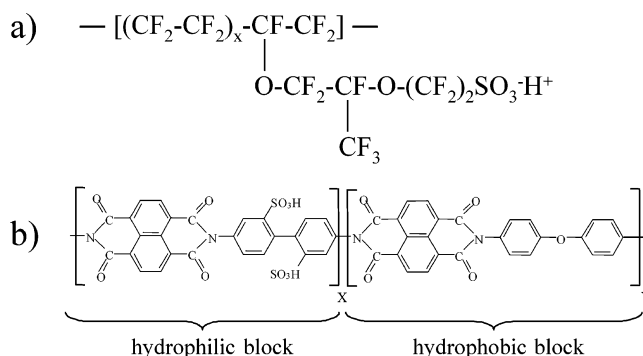


**Figure 1.** (a) Nafion 112 ( $X = 7$ , IEC = 0.91 mequiv/g) and (b) sulfonated polyimide 5/5 ( $X = 5$ ,  $Y = 5$ , IEC = 1.98 mequiv/g).

cost, low glass transition temperature  $T_g$ ) that strongly encourage the development of alternative and competitive materials. Polyaromatic compounds, such as sulfonated polyimides (Figure 1b), are one of these new promising systems with lower cost synthesis and highly tunable properties through a wide choice of chemical units.<sup>1,2</sup> Up to now, their major drawback comes from their fast chemical degradation and the necessity to use weakly charged polymers to minimize the chain hydrolysis.<sup>3</sup> As a result, their conductivity does not compete with that of Nafion, although their ability to allow efficient proton conduction across the material has been demonstrated. At low relative humidity (RH), the macroscopic conductivity of Nafion is much higher than that of sulfonated polyimides. Roughly speaking, 5 water molecules per ionic site ( $\lambda \approx 5$ , RH > 70%) are required to obtain significant macroscopic conductivity in polyimide membranes.<sup>4,5</sup> A comparative analysis of Nafion and sulfonated polyimide transport properties is needed to understand their specific performances and identify valuable hints for further development of competitive membranes. From this point of

\* Authors to whom correspondence should be addressed. Phone: +33 4 38 78 32 85. Fax: +33 4 38 78 56 91. E-mail: perrin@drfmc.ceng.cea.fr.

<sup>†</sup> Structures et Propriétés d'Architectures Moléculaires, UMR 5819.

<sup>‡</sup> Laboratoire de Physique de la Matière Condensée, UMR 7643 du CNRS.

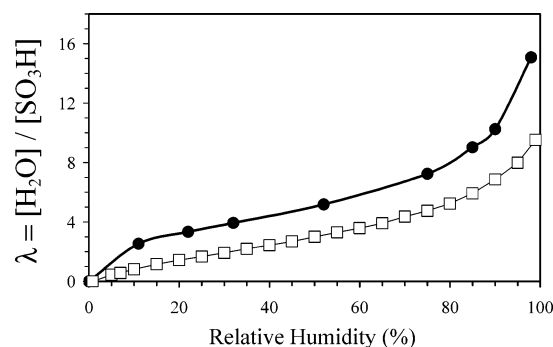


**Figure 2.** Nafion 112 (●) and sulfonated polyimide 5/5 (□) sorption isotherms. The mass variation as a function of the relative humidity has been measured and translated into the number of water molecules per ionic group  $\lambda$  (supposing that  $\lambda = 0$  for dry membranes).

view, the sorption isotherms (Figure 2) do not allow the materials to be significantly differentiated. Moreover, though many structural studies have been performed on both of them,<sup>1,6–11</sup> the structure to transport interdependence relationship has not been clarified up to now. Retrieving information about the molecular dynamical mechanisms involved in water diffusion and proton conduction through confining polymer matrixes of different geometries is compulsory to achieve deeper understanding.

The ionomer membranes exhibit a nanoscale separation between hydrophilic and hydrophobic domains,<sup>12</sup> creating a multiconnected “pore” network available for water sorption. In such complex nanostructured systems, the proton conduction mechanisms should be investigated in a wide range of correlation times, from the molecular level to the macroscopic scale, which requires the combination of complementary techniques.<sup>13</sup> The local molecular dynamics inside a pore network or near the interfacial region is usually probed at short times and distances ( $t < 10$  ns,  $r < 5$  nm) by quasi-elastic neutron scattering (QENS) and neutron spin-echo spectroscopy. A recent QENS study has reported the residence time, the mean jump length, and the self-diffusion coefficient of the water molecules in the Nafion as a function of hydration level,<sup>14</sup> reflecting an increased water mobility tending toward bulklike behavior when increasing the water content. Pulsed-field gradient NMR and other macroscopic experiments such as radiotracer diffusion, used to explore very long times and large distances ( $t > 1$  ms,  $r > 1$   $\mu$ m), have been employed to measure the macroscopic diffusion coefficients in hydrated membranes.<sup>13,15</sup> However, the gap between molecular and macroscopic levels has not been covered; no experimental investigation of the proton motion at the intermediate mesoscopic scale ( $10$  ns  $< t < 0.1$  ms) has been reported yet. One of the few techniques available in this intermediate region is field-cycling nuclear magnetic relaxation.<sup>16</sup> In this paper, we report the first results obtained by NMR relaxometry on Nafion and polyimide membranes equilibrated at various relative humidities (from almost dry to saturated), and more especially we show the ability of the NMR dispersion technique to probe specific transport mechanisms of water molecules associated with wetting or nonwetting properties of the polymer backbone.

### NMR Relaxometry

The spin–lattice relaxation rate  $R_1 = 1/T_1$ , where  $T_1$  accounts for the longitudinal relaxation time, is a NMR quantity sensitive to the rate and the nature of molecular motions. Fast field-cycling NMR<sup>16</sup> stands out from standard NMR usually performed at a fixed frequency. It is a technique where the magnetic

field  $B$  can be tuned to record the longitudinal relaxation rate  $R_1$  over a large range of Larmor frequencies  $\nu = \gamma B/2\pi$ , where  $\gamma$  is the magnetogyric ratio of the nucleus.  $R_1(\omega = 2\pi\nu)$  is called the NMR dispersion (NMRD).

The NMRD law  $R_1(\omega)$  is directly related to the molecular dynamics through the fluctuating magnetic interactions experienced by the nuclear spins carried by the molecules. We focus in this work on the proton–proton dipolar interactions of water molecules and quadrupolar interactions in deuterated water. The interaction fluctuations originate from the orientational (intramolecular dipolar and quadrupolar interactions) and distance fluctuations (intermolecular dipolar interactions). The relaxation rate  $R_1(\omega)$  may be written as

$$R_1(\omega) = A[J_1(\omega) + 4J_2(2\omega)] \quad (1)$$

with

$$J_m(\omega) = \int_{-\infty}^{+\infty} G_m(t) e^{-i\omega t} dt \quad (2)$$

and

$$G_m(t) = \langle Y_{2,m}^*(0) Y_{2,m}(t) \rangle \quad (3)$$

where  $G_m(t)$  is the self-correlation function of the spherical harmonics  $Y_{2,m}$  ( $m = 0, \pm 1, \pm 2$ ) associated with the H–H and O–D vectors in the laboratory frame with  $B$  along the  $z$ -axis.  $A$  is a prefactor depending on specific spin interactions.

The reorientation processes of small fluid molecules in the bulk state are very fast ( $\sim 10^{-12}$  s). When the fluid is entrapped in a matrix and thus confined, the existence of accessible solid surfaces implies that the reorientations are strongly slowed by temporary adsorption/desorption steps of the molecules onto the surface, diffusion along the surface, exchange with the bulk phase, and translational diffusion in the bulk phase. Long correlation times are thus introduced in the autocorrelation function, giving rise to strong enhancement of  $R_1(\omega)$  at low frequencies. The frequency range usually accessible with a relaxometer (10 kHz to 20 MHz) allows dynamical correlation times on the order of  $10^{-5}$  s to be reached, i.e.,  $10^7$  times slower than the characteristic time of bulk water reorientations.

Typically, a fluid molecule experiencing dynamical fluctuations within the Larmor frequency range of the relaxometer will be characterized by a  $\omega$ -dependent relaxation rate  $R_1$ . Fast and isotropic motions of small molecules characterized by typical correlation times  $\tau_c$  on the order of few picoseconds lead to flat  $R_1(\omega)$  profiles with a magnitude proportional to the correlation time. For instance, the bulk water relaxation rate  $R_1$  is expected to be constant and roughly equal to  $0.3$  s $^{-1}$  over the whole spectral window from 10 kHz to 20 MHz.

The sensitivity of NMR relaxometry to surface effects makes it a particularly powerful tool to investigate fluid dynamics in confinement.<sup>17,18</sup> A detailed analysis of the shapes and magnitudes of the NMRD profiles is not straightforward in complex systems, as it is necessary to identify the contribution of each process responsible for the molecules slowing in a confined situation—the orientational anisotropy degree at each adsorption site, kinetics of the adsorption/desorption process, translational diffusive modes near the surface, exchange between an adsorbed layer and the bulk phase, and the topology of the matrix. A comparison with some cases where an analytical expression of  $R_1(\omega)$  is available is a useful guide. In our case, we refer to the work done on the wetting or nonwetting behavior of liquids embedded in porous materials.<sup>17–20</sup>

## Experimental Section

**Materials.** Membranes that are 50- $\mu\text{m}$ -thick have been used in this work. Nafion membranes with an ionic exchange capacity (IEC) of 0.9 mequiv/g (i.e., 0.9 mmol of  $\text{SO}_3\text{H}$  per gram of polymer) and a density about 2.1  $\text{g}/\text{cm}^3$  have been chosen (Nafion 112, Figure 1a). In the case of polyimides, the polymers are composed of a hydrophilic sulfonated block based on a naphthalenic structure and an hydrophobic block obtained with an oxydianiline monomer (Figure 1b). The repetition rate of the blocks is 5/5 ( $X = 5$  and  $Y = 5$ ), corresponding to an IEC of 1.98 mequiv/g for a polymer density close to 1.4  $\text{g}/\text{cm}^3$ . If  $n_s$  is the number of sulfonated groups and  $n_p$  the total number of polar groups (including, for instance, carbonyl groups that are present in the polyimides), then the ratio defined as  $f_s = n_s/n_p$  is a chemical characteristic of each polymer (in the case of a fully perfluorinated polymer such as Nafion 112,  $f_s = 1$ ). The ratio  $\lambda = N/n_s$ , with  $N$  the total number of water molecules in the material, characterizes the hydration state.

**Sample Preparation.** The Nafion 112 membranes were purchased from Dupont Company. Strips of 0.7-cm-wide Nafion were cut from the raw sheet. To ensure a complete acidification they were soaked in 800 mL of 2 mol/L hydrochloric acid solution at 80 °C for 2 h and rinsed in distilled–deionized water at 80 °C for 2 h. They were then soaked in 800 mL of 1 mol/L nitric acid solution at 80 °C for 2 h and rinsed in distilled–deionized water at 80 °C for 2 h. Paramagnetic impurities introduced during the manufacture of Nafion have been removed by applying a cleaning protocol close to the one described by MacMillan et al.<sup>21</sup> The purification was achieved by chelation with ethylenediaminetetraacetic acid (EDTA). The strips are soaked in 0.015 mol/L EDTA at room temperature for 1 day and rinsed in distilled–deionized water at 80 °C for 2 h. This step was repeated two times. The efficiency of the protocol has been checked by electronic paramagnetic resonance.

The sulfonated polyimide membranes were provided by the LMOPS laboratory (Vernaison, France). Strips of sulfonated polyimide were soaked in 500 mL of 0.5 mol/L sulfuric acid solution at room temperature for 4 h. They were then soaked in distilled–deionized water at 50 °C for 4 h and rinsed with fresh distilled water.

Nafion and sulfonated polyimide strips were rolled inside 10-mm-diameter NMR tubes (typical weight of one sample in the dry state is 500 mg). A series of samples at different water contents have been prepared by controlling the relative humidity (RH) inside the NMR tube. For doing so, a small glass tube containing well-chosen saturated salt solutions has been placed above the membrane in the 10-mm-diameter tube. The nature of the salt fixes the vapor pressure  $P/P_0$  at room temperature and thus imposes a known RH that can be translated into  $\lambda$  through the sorption isotherms (Table 1). The NMR tube being closed, it has been necessary to wait for several weeks until the equilibrium was achieved at the desired RH, which we have controlled by measuring the amplitude of the magnetization at a given fixed magnetic field as a function of time; the NMR relaxometry measurements were performed when the equilibrium plateau was reached for all samples.

**NMR Relaxometry Experiments.**  $^1\text{H}$  NMRD and  $^2\text{H}$  NMRD experiments related to water molecules inside the membranes have been performed at 298 K with a Stellar Spinmaster-FFC2000 relaxometer. Each measurement is generally a three-

**TABLE 1: Salts Used for the Preparation of Saturated Solutions at Room Temperature, together with the Corresponding Values of Relative Humidities and  $\lambda$  (Number of Water Molecules per Ionic Site), for Nafion and Polyimide Membranes<sup>a</sup>**

salt	RH	$\lambda_{\text{nafion}}$	$\lambda_{\text{polyimide}}$
LiCl	11%		1
KCOOCH <sub>3</sub>	22%	3.7	1.5
MgCl <sub>2</sub>	32%		2.1
Mg(NO <sub>3</sub> ) <sub>2</sub>	52%	5.6	3.1
NaCl	75%		4.8
KCl	85%		5.9
BaCl <sub>2</sub>	90%	10.6	6.9
water	100%		9.5
	in liquid water		18

<sup>a</sup> One polyimide membrane also has been immersed in liquid water to obtain a swelling of  $\lambda = 18$  (see ref 1).

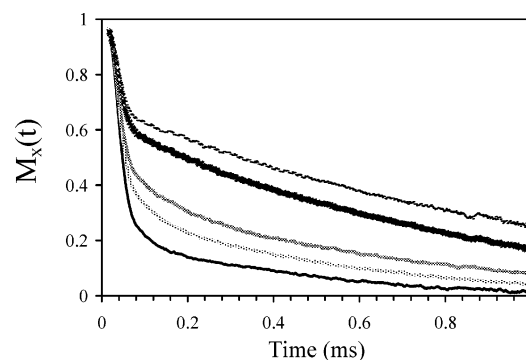


**Figure 3.** Free induction decay of the magnetization measured on the sulfonated polyimide 5/5 at different water contents, showing the fast solid component and the slow water component. The magnetization amplitudes in the relaxometry experiments have been recorded at  $t > 0.15$  ms. From top to bottom: 90%, 85%, 52%, 32%, and 11% RH.

step cycle: polarization/relaxation/detection. The polarization field ( $B_p = 0.47$  T,  $\nu_p = 20$  MHz for protons) creates an observable macroscopic magnetization. It is then quickly switched to a much lower value ( $23 \text{ mT} < B_r < 0.2$  T) at which the relaxation takes place. The detection of the magnetization value after a given relaxation time  $t_r$  is derived from the amplitude of the free induction decay (FID) recorded after a standard  $\pi/2$  pulse at a fixed intermediate field ( $B_d = 0.3$  T,  $\nu_d = 12.8$  MHz for protons). This measure is repeated to obtain a series of FIDs as a function of time  $t_r$ . The relaxation time  $T_1(\omega_r)$  is extracted from the exponential variation of the FID amplitude with  $t_r$ . For relaxation fields between 0.2 and 0.47 T, the polarization step is not necessary.

## Results and Discussion

**Sulfonated Polyimides.** The polymer matrix of the sulfonated polyimides is protonated, which implies to separate in the  $^1\text{H}$  NMR signal the contribution arising from the matrix from that of the water. The FID exhibits two components easily disclosed: a very fast decay, due to the solid matrix, followed by a much slower one due to water (Figure 3). The water NMRDs have been obtained by recording the FIDs in the time window relative to the water signal only, and its spin–lattice relaxation is found to be monoexponential.

Figure 4a shows the  $R_1(\omega)$  profiles obtained on the polyimide 5/5 as a function of the relative humidities, from almost dry (11% RH) to fully saturated (100% RH). At all relative humidities, a strong  $R_1(\omega)$  dispersion is observed, following a  $\omega^{-a}$  trend with  $a$  close to 0.5. As shown elsewhere,<sup>22</sup> this is the signature of a noticeable interaction between the entrapped fluid



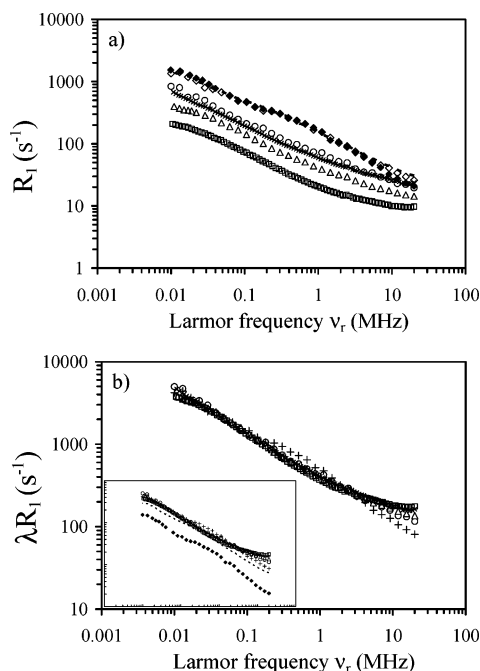


**Figure 4.** (a) Dispersion law  $R_1(\omega)$  for the sulfonated polyimide 5/5 at room temperature, at different humidities: 11% ( $\blacklozenge$ ), 32% ( $\circ$ ), 52% ( $\diamond$ ), 85% ( $\circ$ ), 90% ( $\times$ ), 100% ( $\triangle$ ), and immersed in water ( $\square$ ). (b) The same data (same symbols are used for the different hydration degrees) in the reduced coordinate  $\lambda R_1(\omega)$  show the existence of a master curve at RH > 52%. In the inset, deviation from the master curve is observed for hydrated polyimides at 11% and 32% RH.

and the polymeric interface, typical of a good wetting. Below 52% RH, the dispersion curves are superimposed. A strong shift is observed at a higher water content ( $\lambda = 5.9$ – $9.5$ , and  $\lambda = 18$  that corresponds to the membrane immersed in liquid water). In this regime, it is possible to obtain a master curve  $\lambda R_1(\omega)$ , as shown in Figure 4b.

Such a behavior can be rationalized according to the hydration mechanisms derived from infrared absorption spectroscopy measurements.<sup>23</sup> A two-step water uptake has been proposed. Up to 70% RH, a local hydration of ionic and polar groups of the polyimide chains leads to disconnected water clusters. The number of adsorbed water molecules increases up to its limit value  $N_a$ . Above 70%, a continuous hydrogen bond water network develops with  $N_a$  staying constant. Our NMRD data are consistent with this hydration scenario. At low hydration levels, an increasing number of small and disconnected water clusters generates similar relaxation processes, leading to a unique  $R_1(\omega)$  profile. It has been mentioned previously that no significant conductivity is observed before  $\lambda \approx 5$  in these materials, which also supports the idea that in the early stage of hydration the percolation threshold is not reached and no continuous path is available until the first water layer has been adsorbed onto the whole surface. Above the threshold, interconnections between isolated clusters induce a rapid exchange between water molecules adsorbed on polar groups and “bulky” water. When  $p_a = N_a/N$  and  $p_b = (N - N_a)/N$  are introduced, the relaxation rate within the scheme of fast exchange<sup>24</sup> can be written as

$$R_1(\omega) = p_a R_1^a(\omega) + p_b R_1^b(\omega) \quad (4)$$

where  $R_1^a(\omega)$  is the relaxation rate of the adsorbed phase and  $R_1^b(\omega)$  that of the bulky phase. When the constant number of adsorbed water molecules per polar group  $N_H = N_a/n_p$  is

introduced, eq 4 can be expressed as

$$R_1(\omega) = \frac{N_H}{\lambda f_s} (R_1^a(\omega) - R_1^b(\omega)) + R_1^b(\omega) \quad (5)$$

Experiments show that the quantity  $\lambda R_1(\omega)$  is independent of the hydration level at low frequencies (Figure 4b), which corresponds to the case  $R_1^a(\omega) \gg R_1^b(\omega)$  leading to

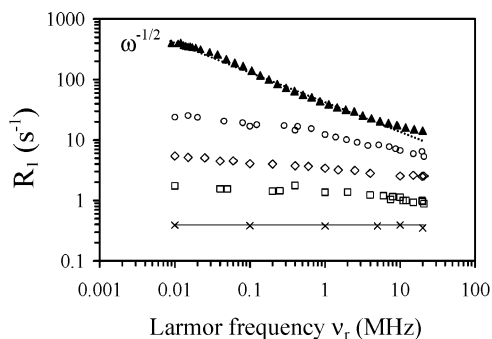
$$\lambda R_1(\omega) \approx \frac{N_H}{f_s} R_1^a(\omega) \quad (6)$$

In summary, the observation of strongly dispersed NMRD profiles at all hydration levels reveals a strong interaction between the water molecules and the polyimide matrix. The  $1/\sqrt{\omega}$  dispersion law looks very similar to what has been observed in rigid porous media such as Vycor glass<sup>19,24</sup> where the nuclear relaxation is mainly driven by reorientations mediated by diffusional translations. However, as the interfacial region is diffuse rather than sharp in the polyimide membranes,<sup>1,25</sup> no definitive conclusions concerning the molecular origin of the relaxation can be proposed. Experiments on deuterated water are currently under investigation in our laboratory to evaluate the respective contributions of translational and reorientational dynamics (inter-dipolar and intra-dipolar interactions).

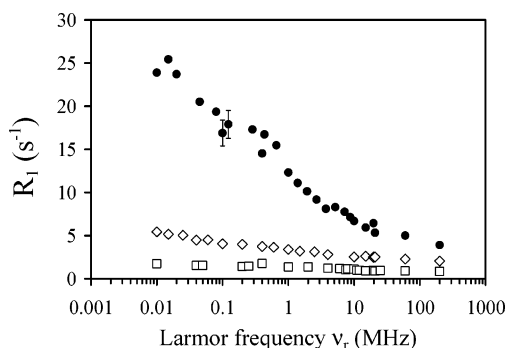
**The Nafion Membrane.** The Nafion polymer being perfluorinated, in the Nafion–water system the <sup>1</sup>H NMR signal arises only from water, and the FID has one component. The longitudinal relaxations are monoexponential and characterized by a single  $T_1$  at each frequency. The fast field-cycling NMRD profiles have been extended at higher frequencies by performing experiments on standard spectrometers operating at fixed frequencies (Bruker Minispec 20 and 60 MHz, Bruker Avance 200 MHz, and Varian Unity 400 MHz). The longitudinal and transverse relaxation times of the membranes (<sup>19</sup>F nucleus) have been measured at 20 MHz to check the eventuality of a direct <sup>19</sup>F–<sup>1</sup>H dipolar interaction between the polymer chains and the water molecules. The <sup>19</sup>F longitudinal relaxation time  $T_1$  appears to be hydration-independent and equal to 350 ms; its transverse relaxation time  $T_2$  is also constant (on the order of 50  $\mu$ s), while that of the protons ranges from 65 to 650 ms when increasing the hydration in the Nafion membrane. Thus, no direct and strong dipolar interaction between fluorine atoms and water protons was found (local nonwetting situation), which is also supported by the similar temperature dependences of the proton longitudinal relaxation time  $T_1$  measured in water and in hydrated Nafion.<sup>21</sup>

Figure 5 shows the  $R_1(\omega)$  profiles obtained on the Nafion for three different hydration levels:  $\lambda = 3.7$ ,  $\lambda = 5.6$ , and  $\lambda = 10.6$ , together with the NMRD signals of bulk water and fully hydrated sulfonated polyimides (RH 100%,  $\lambda = 9.5$ ). The longitudinal relaxation rates in the Nafion are still higher than that of bulk water, due to confinement, even if this effect is much less pronounced than in the polyimides.

In comparison to the sulfonated polyimide profile, the Nafion exhibits at all hydration levels a less pronounced frequency dependence, which is the signature of the nonwetting situation and weak surface interactions.<sup>22</sup> As seen from this figure, NMR relaxometry measurements allow efficient discrimination of the water behavior in nonwetting membranes such as Nafion from that in wetting ones such as polyimides.



**Figure 5.** Dispersion of the relaxation rate  $R_1$  as a function of the NMR frequency at 298 K, for fully hydrated polyimide 5/5 ( $\blacktriangle$ ) and Nafion 112 at  $\lambda = 3.7$  ( $\circ$ ), 5.6 ( $\diamond$ ), and 10.6 ( $\square$ ). The frequency-independent signal from bulk water is also shown ( $\times$ ).



**Figure 6.** Semilog representation of the  $^1\text{H}$  NMRD  $R_1(\omega)$  profiles (measured by fast field-cycling relaxometry and completed at high frequency on standard NMR spectrometers) of the Nafion 112 at  $\lambda = 3.7$  ( $\bullet$ ), 5.6 ( $\diamond$ ), and 10.6 ( $\square$ ).

At low hydration  $\lambda = 3.7$ , the  $\omega$ -dependence follows a logarithmic trend that is progressively replaced by a plateau as  $\lambda$  increases (Figure 6). Logarithmic NMRD profiles are found in the case of dipolar relaxation by translational diffusion (interdipolar interactions) of a nonwetting liquid confined in a two-dimensional (2D) porous media.<sup>26</sup> To evaluate the relevance of such a model in the case of less hydrated Nafion, it is necessary to separate the inter- and the intramolecular contributions to the dipolar relaxation.

To do so, we have performed  $^2\text{H}$  NMRD experiments on the same Nafion membrane and at the same water content as for the  $^1\text{H}$  experiments. The spin–lattice relaxation of the deuterium nucleus arises from the fluctuation of the quadrupolar interaction between the spin and the electric field gradient along the O–D bond. This intense quadrupolar interaction being intramolecular, the relaxation rate  $R_{1,Q}(\omega)$  reduces to the orientational correlation function of the water molecule. Moreover, in the case of a spin equal to 1, the quadrupolar relaxation rate  $R_{1,Q}(\omega)$  obeys the same equation as the one associated with the intramolecular contribution of the dipolar H–H relaxation (eq 1). We have thus

$$R_1(\omega) = A[J_1(\omega) + 4J_2(2\omega)] \quad (7)$$

with  $A$  and  $\omega$  in the case of intramolecular dipolar H–H interaction (i) and deuterium quadrupolar interaction (ii) given by

$$(i) \quad \omega = \omega_H \quad \text{and} \quad A = \frac{3}{20} \left[ \frac{\gamma_H^2 \hbar^2}{b^3} \right]^2 \quad (8)$$

$$(ii) \quad \omega = \omega_{\text{deut}} = \frac{\gamma_{\text{deut}}}{\gamma_H} \omega_H \approx \frac{\omega_H}{6.51} \quad \text{and}$$

$$A = \frac{3\pi^2}{20} \chi^2 \left( 1 + \frac{\eta^2}{3} \right) \quad (9)$$

For the water molecule,  $b$  is the H–H distance equal to 1.51 Å,  $\chi$  the coupling constant is equal to  $260 \pm 10$  kHz, and  $\eta$  the asymmetry coefficient is equal to 0.11.<sup>27</sup>

As a consequence, the intramolecular contribution to the proton relaxation rate  $R_1(\omega)$  can be obtained from the measurement of deuterium relaxation through

$$R_1^{\text{intra}}(\omega) = \frac{(\gamma_H^2 \hbar)^2}{\pi^2 \chi^2 \left( 1 + \frac{\eta^2}{3} \right) b^6} R_{1,Q}(\omega) = 7.11 \times 10^{-2} R_{1,Q}(\omega) \quad (10)$$

The NMRD profile of the intermolecular dipolar contribution to the proton relaxation is easily obtained as

$$R_1^{\text{inter}}(\omega) = R_1(\omega) - R_1^{\text{intra}}(\omega) \quad (11)$$

Figure 7 shows the deuterium NMRD profile  $R_{1,Q}(\omega)$ , and Figure 8 the intermolecular dipolar contribution  $R_1^{\text{inter}}(\omega)$  for the three hydrated samples. Close inspection of Figure 8 confirms that  $R_1^{\text{inter}}(\omega)$  evolves logarithmically at low water content, thus suggesting that Korb's model is relevant and that the proton translational dynamics is essentially a 2D diffusional process in the microsecond time range. The existence of such

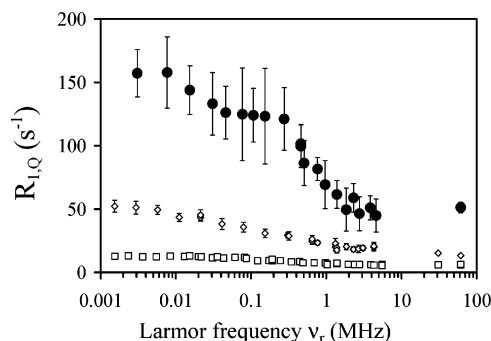


**Figure 7.** Semilog representation of the  $^2\text{H}$  NMRD  $R_{1,Q}(\omega)$  profiles (measured by fast field-cycling relaxometry and completed at high frequency on standard NMR spectrometers) of the Nafion 112 at  $\lambda = 3.7$  ( $\bullet$ ), 5.6 ( $\diamond$ ), and 10.6 ( $\square$ ).

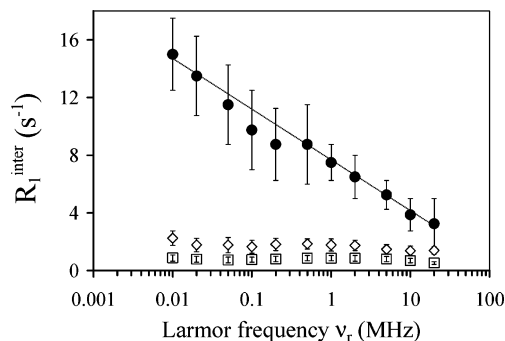


**Figure 8.** Semilog representation of the inter-dipolar contribution to the proton relaxation obtained by subtracting (eq 11) the intramolecular contribution (calculated from the deuterium profiles and eq 10) from the total proton relaxation of the Nafion 112 at  $\lambda = 3.7$  ( $\bullet$ ), 5.6 ( $\diamond$ ), and 10.6 ( $\square$ ). The line is a guide to show the logarithmic behavior observed at low water content. At higher hydration, the inter-dipolar relaxation dispersions are almost flat.

a bidimensional geometry at very low water content is consistent with recent structural observations on the Nafion membrane. A dilution law close to  $\phi^{-1}$  ( $\phi$  being the polymer volume fraction), typical of one-dimensional swelling of biaxial polymeric aggregates, has been reported in the  $\lambda$  range of our study.<sup>11,28</sup> These elongated hydrophobic aggregates embedded in a continuous ionic medium are assembled into bundles<sup>8</sup> with a typical size of 80 nm. Interesting enough, taking into account the water self-diffusion coefficient obtained by QENS<sup>14</sup> at  $\lambda = 4$  and the former bundle nominal size, the corresponding correlation time of 2D self-diffusion is about 10  $\mu$ s, and the associated frequency of a few tenths of a kilohertz falls in the low-frequency range of our NMRD logarithmic profile.

The drastic change in the  $R_1(\omega)$  shape observed with a weak water uptake ( $\lambda$  increasing from 3.7 to 5.6) can be understood also through the model of ref 26, which predicts that a weak increase of pore size induces rapid disappearance of the bidimensional behavior and the emergence of a plateau related to three-dimensional diffusion (Figure 2 in ref 26). These NMRD properties could be linked to the structural characteristic distances of the system. In the biaxial dilution regime, the correlation distance between elongated aggregates can be associated to a lamellar spacing proportional to  $\lambda$  in the hydration range of this study. Such a spacing, on the order of a nanometer at  $\lambda = 10.6$  (i.e., a few water layers), decreases such that the isotropic to anisotropic diffusion transition can take place when drying the membrane.

## Conclusions

We have performed NMR relaxometry experiments on two kinds of ionomer membranes: Nafion and sulfonated polyimide. Our preliminary results indicate that the technique is well adapted to the study of water dynamics in these hydrated systems in the range of a few nanometers and can provide valuable information to discriminate the molecular mechanisms associated with water motion as a function of the hydration state. Although the two materials are thought to answer the same specifications for PEFC applications, we have shown that they exhibit significantly different  $R_1(\omega)$  signatures. In the case of polyimides, strong dispersions characteristic of good wetting have been observed. Our results confirm the infrared description of a two-step hydration process, with a strong interaction between water and the polymer chains. A large amount of water is required to build the first hydration layer necessary for enabling long-range transport. Then, the rapid exchange between the adsorbed water phase and the bulky phase shows up through the appearance of a master curve showing the proportionality between the NMRD profiles and  $1/\lambda$ . Such a behavior, together with the observation of the  $1/\sqrt{\omega}$  law at each water content, is typical of rigid porous media in wetting conditions.

In the Nafion, the situation looks very different. The nonwetting behavior of the perfluorinated membrane has been shown at the microsecond scale through the observation of poorly dispersive relaxation rates. Moreover, a transition from 2D to 3D local diffusion when increasing the water content is

consistent with the evolution of the intermolecular dipolar NMRD. The anisotropy of diffusion observed at a low hydration level could be related to a local structural organization involving biaxial aggregates organized in lamellar domains at the nanometer scale. Molecular dynamics simulation and elaboration of a theoretical model are required at this stage to further interpret the experimental data here reported. These studies are presently underway in our laboratory.

**Acknowledgment.** We acknowledge O. Diat, G. Gebel, Y. Maréchal, and F. Volino for very helpful discussions about membrane properties and NMR relaxation. We thank Professor J.-P. Cohen-Addad (Laboratoire de Spectrométrie Physique, Grenoble, France) for the access to the Bruker Minispec Analyzers and the Magnetic Resonance Center of Grenoble (CGRM) for the access to the Bruker Advance and Varian Unity spectrometers.

## References and Notes

- (1) Cornet, N.; Diat, O.; Gebel, G.; Jousse, F.; Marsacq, D.; Mercier, R.; Pineri, M. *J. New Mater. Electrochem. Syst.* **2000**, *3*, 33.
- (2) Genies, C.; Mercier, R.; Sillion, B.; Cornet, N.; Gebel, G.; Pineri, M. *Polymer* **2001**, *42*, 359.
- (3) Genies, C.; Mercier, R.; Sillion, B.; Petiaud, R.; Cornet, N.; Gebel, G.; Pineri, M. *Polymer* **2001**, *42*, 5097.
- (4) Asano, N.; Miyatake, K.; Watanabe, M. *Chem. Mater.* **2004**, *16*, 2841.
- (5) Yin, Y.; Fang, J.; Watari, T.; Tanaka, K.; Kita, H.; Okamoto, K. *J. Mater. Chem.* **2004**, *14*, 1062.
- (6) Blachot, J.-F.; Diat, O.; Putaux, J.-L.; Rollet, A.-L.; Rubatat, L.; Vallois, C.; Müller, M.; Gebel, G. *J. Membr. Sci.* **2003**, *214*, 31.
- (7) Rubatat, L.; Rollet, A.-L.; Gebel, G.; Diat, O. *Macromolecules* **2002**, *35*, 4050.
- (8) Rubatat, L.; Gebel, G.; Diat, O. *Macromolecules* **2004**, *37*, 7772.
- (9) Kreuer, K. D. *J. Membr. Sci.* **2001**, *185*, 29.
- (10) Gierke, T. D.; Munn, G. E.; Wilson, F. C. *J. Polym. Sci., Polym. Phys. Ed.* **1981**, *19*, 1687.
- (11) Litt, M. H. *Polym. Prepr. (Am. Chem. Soc., Div. Polym. Chem.)* **1997**, *38*, 80.
- (12) Schlick, S. *Ionomers: Characterization, Theory and Applications*; CRC Press: Boca Raton, FL, 1996.
- (13) Rollet, A.-L.; Simonin, J.-P.; Turq, P.; Gebel, G.; Kahn, R.; Vandais, A.; Noël, J.-P.; Malveau, C.; Canet, D. *J. Phys. Chem. B* **2001**, *105*, 4503.
- (14) Pivovar, A. M.; Pivovar, B. S. *J. Phys. Chem. B* **2005**, *109*, 785.
- (15) Zawodzinski, T. A.; Neeman, M.; Sillerud, L. O.; Gottesfeld, S. *J. Phys. Chem.* **1991**, *95*, 6040.
- (16) Noack, F. *Prog. Nucl. Magn. Reson. Spectrosc.* **1986**, *18*, 171.
- (17) Kimmich, R. *NMR Tomography Diffusometry Relaxometry*; Springer: Berlin, 1997.
- (18) Kimmich, R.; Anoardo, E. *Prog. Nucl. Magn. Reson. Spectrosc.* **2004**, *44*, 257.
- (19) Levitz, P. E. *Magn. Reson. Imaging* **2003**, *21*, 177.
- (20) Levitz, P.; Korb, J.-P. *Europhys. Lett.* **2005**, *70*, 684.
- (21) MacMillan, B.; Sharp, A. R.; Armstrong, R. L. *Polymer* **1999**, *40*, 2471.
- (22) Stapf, S.; Kimmich, R.; Seitter, R.-O. *Phys. Rev. Lett.* **1995**, *75*, 2855.
- (23) Jamroz, D.; Maréchal, Y. *J. Phys. Chem. B* **2005**, *109*, 19664.
- (24) Mattea, C.; Kimmich, R.; Ardelean, I.; Wonorahardjo, S.; Farrher, G. *J. Chem. Phys.* **2004**, *121*, 10648.
- (25) Rollet, A.-L.; Diat, O.; Gebel, G. *J. Phys. Chem. B* **2004**, *108*, 1130.
- (26) Korb, J.-P.; Xu, S.; Jonas, J. *J. Chem. Phys.* **1993**, *98*, 2411.
- (27) Hardy, E. H.; Müller, M. G.; Vogt, P. S.; Bratschi, C.; Kirchner, B.; Huber, H.; Searles, D. J. *J. Chem. Phys.* **2003**, *119*, 6184.
- (28) Gebel, G. *Polymer* **2000**, *41*, 5829.